GEOPHYSICAL RESEARCH LETTERS, VOL. 23, NO. 7, PAGES 729-732, APRIL 1, 1996

Satellite-based identification of linked vegetation index and sea surface temperature anomaly areas from 1982-1990 for Africa, Australia and South America

Ranga B. Myneni

Department of Geography, University of Maryland and Biospheric Sciences Branch, NASA Goddard Space Flight Center, Greenbelt, Maryland

Sietse O. Los

Science Systems Applications Inc. and Biospheric Sciences Branch, NASA Goddard Space Flight Center, Greenbelt, Maryland

Compton J. Tucker

Biospheric Sciences Branch, NASA Goddard Space Flight Center, Greenbelt, Maryland

Abstract. Meteorological satellite data from 1982 to 1990 were used to identify areas of significant association between tropical Pacific sea surface temperature (SST) and remotely sensed normalized difference vegetation index (NDVI) anomalies, here taken as a surrogate for rainfall anomalies. During this period, large areas of arid and semi-arid Africa, Australia and South America experienced NDVI anomalies directly correlated to tropical Pacific SST anomalies. The results are limited by the relatively short time period of analysis. However, they confirm the disruptive effects of large-scale tropical Pacific SST variations on arid and semi-arid continental rainfall patterns in Africa, Australia, and South America, as reported previously.

Introduction

Several workers have compared surface precipitation patterns with El Niño Southern Oscillation cycle sea surface temperature (SST) anomalies, identifying areas where rainfall anomalies were correlated with tropical Pacific SST anomalies [*McBride and Nicholls, 1983; Ropelewski and Halpert, 1987; 1989*]. Point rainfall frequently does not adequately represent areal rainfall, especially in semi-arid tropical regions where rainfall is often erratically distributed. Thus accurate estimates of the geographical extent of SST linked precipitation anomalies has been hampered in many areas. We have used satellite-derived normalized difference vegetation index (NDVI), which several studies have shown to be highly correlated with arid and semi-arid rainfall [*Malo and Nicholson, 1990; Nicholson et al., 1990; Tucker et al., 1991*]. Our approach has been to correlate tropical Pacific SST anomalies from the NINO3 region (5° S to 5° N latitude and 90° W to 150° W longitude) and NDVI anomalies, thus delineating anomalous rainfall areas through direct measurement of vegetation amount and condition in a spatially continuous manner for arid and semi-arid Africa, South America, and Australia.

Copyright 1996 by the American Geophysical Union.

Paper number 96GL00266
0094-8534/96/96GL-00266$03.00

Data and Methods

The National Oceanic and Atmospheric Administration's polar-orbiting meteorological satellites obtain daily global information from the advanced very high resolution radiometer (AVHRR) instrument. Data from the AVHRR instrument are used to produce a vegetation index directly related to the density of chlorophyll contained in plants on land [*Sellers, 1985*]. The satellite-sensed vegetation index is expressed as a normalized difference of two channels [(Channel 2 - Channel 1) / (Channel 2 + Channel 1)], where Channel 1 records reflected light from 0.55-0.70 μm and Channel 2 records reflected light from 0.72-1.1 μm. Combining data from these adjacent spectral regions compensates for differences in irradiance and provides an estimate of the intercepted fraction of the photosynthetically active radiation or photosynthetic capacity [*Asrar et al., 1984*]. These data are strongly related to total primary production when summed or averaged over the growing season [*Fung et al., 1987*].

Daily daytime 4-km AVHRR data were used from NOAA-7 (1982 to 1984), NOAA-9 (1985 to 1988), and NOAA-11 (1989 to 1990) covering Africa, Australia, and South America. The eruption of Mt. Pinatubo in mid-1991 injected a

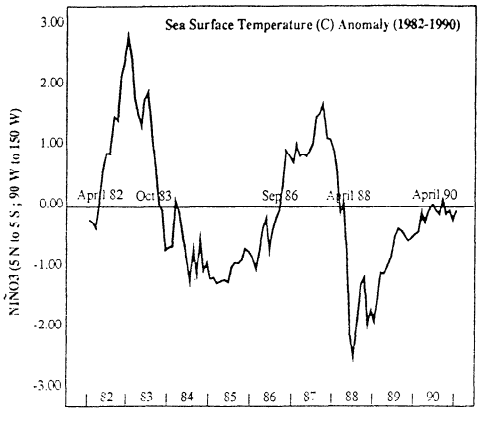

Figure 1. SST anomalies from the tropical Pacific NINO3 area of 5^oS to 5^oN latitude and 90^oW to 150^oW longitude from 1982 to 1990 [*Woodruff et al., 1993*].

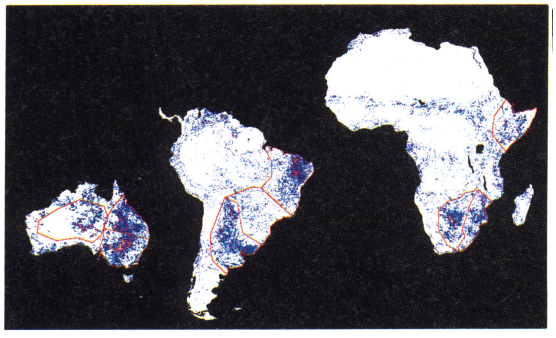

Figure 2. Summary of areas with linked tropical Pacific SST and NDVI anomalies for Africa, Australia and South America. The 1982-90 time period was divided into 4 ENSO events, characterized by a consecutive 12 month period that included the peak SST anomaly and the southern hemisphere summer rainfall period (May 1982 - April 1983; March 1985 - February 1986; March 1987 - February 1988; May 1988 - April 1989). For every land pixel, correlations were performed between NDVI and SST anomalies for each of the 4 events. Areas with 2 occurrences are labeled blue, 3 occurrences are labeled pink, and 4 occurrences are labeled yellow. An occurrence is defined as (1) correlation coefficients greater than $|0.5|$ (2) cumulative twelve month NDVI anomaly greater than 0.3 or lesser than -0.3, and (3) surrounded on all sides by eight similarly pixels. The contours indicate regions from which the time series shown in Figure 5 and the entries in Table 1 were based.

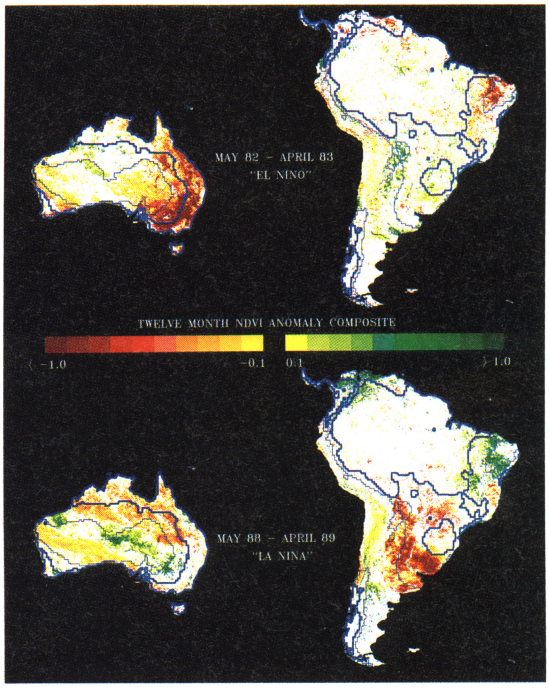

Figure 4. Areas of linked tropical Pacific SST and NDVI anomalies for Australia and South America. The pixels identified are those with SST-NDVI anomaly correlation coefficients greater than $|0.5|$. Thin lines plotted on the South American image are rainfall contours of $\approx$750 mm/year; the bold lines indicate $\approx$1500 mm/year of rainfall. For Australia these contours indicate $\approx$300 and $\approx$500 mm/year of rainfall.

significant quantity of aerosols into the stratosphere which prevented us from using data for 1991 onwards. Data were processed into a maximum value NDVI composite by month which minimizes atmospheric effects, cloud contamination, scan angle effects, and solar zenith angle effects. Data were numerically calibrated to a common reference to permit identification of NDVI anomalies among satellites and have a spatial resolution of $\approx$7.6km [*Los et al., 1994*].

Pacific sea surface temperature anomalies from 5°S to 5°N latitude and 90°W to 150°W longitude were obtained from the Comprehensive Ocean - Atmosphere Data Set program [*Woodruff et al., 1993*]. Monthly mean NDVI was computed and anomalies from each month determined. The similarity between the SST and NDVI monthly anomaly time series was determined, pixel by pixel, by evaluating the cross correlation coefficient using the procedure CORREL outlined in Numerical Recipes [*Press et al., 1986*]. This method identifies land areas where NDVI anomalies are similar to SST anomalies, thus providing direct measurement of location and areal extent of affected arid and semi-arid areas. Our technique is not accurate for areas receiving more than $\approx$1000 mm/yr precipitation as the relationship between NDVI and rainfall tends to saturate.

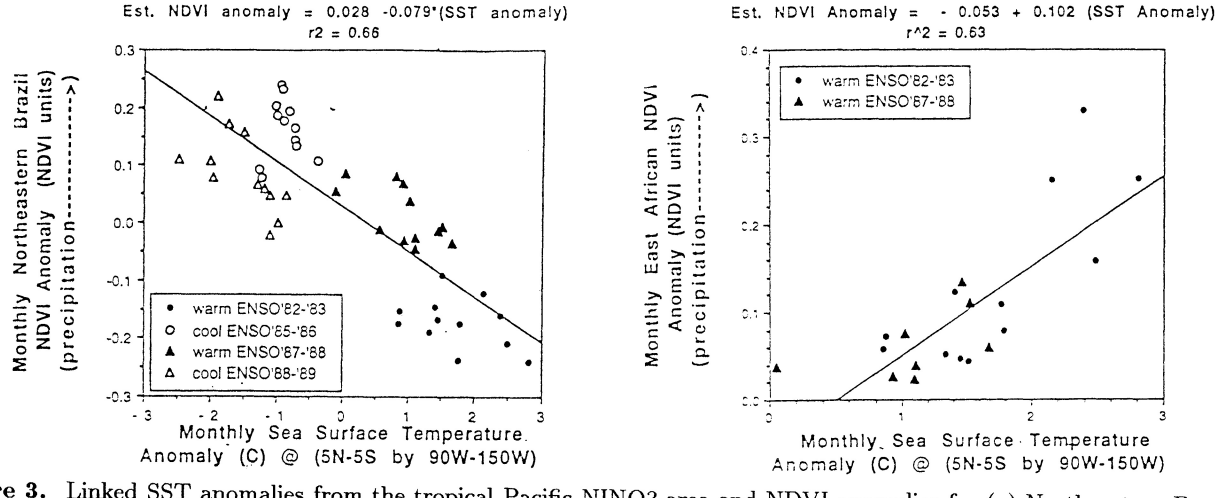

Figure 3. Linked SST anomalies from the tropical Pacific NINO3 area and NDVI anomalies for (a) Northeastern Brazil and (b) Eastern Africa.

Table 1. Areas of Africa, Australia and South America where linked tropical Pacific SST and NDVI anomalies were determined from 1982 to 1990. The areas in this table are the areas where time series correlation coefficients are greater than |0.5| and where the cumulative twelve month NDVI anomaly was greater than 0.3 or lesser than -0.3. The regions are shown in Figure 2.

	ENSO Cycle Sea Surface Warming				ENSO Cycle Sea Surface Cooling			
	May 1982 to Apr 1983		Mar 1987 to Feb 1988		Mar 1985 to Feb 1986		May 1988 to Apr 1989	
Region	+ve NDVI Anomalies	-ve NDVI Anomalies	+ve NDVI Anomalies	-ve NDVI Anomalies	+ve NDVI Anomalies	-ve NDVI Anomalies	+ve NDVI Anomalies	-ve NDVI Anomalies
Northeastern Brazil	83,200	498,600	75,000	360,700	1,001,700	26,500	557,000	82,600
Southeastern S. America	485,100	144,300	406,200	285,200	996,600	105,200	16,500	1,665,800
Eastern Australia	1,000	1,743,500	106,400	499,100	173,100	744,400	201,300	549,900
Central Australia	62,500	39,700	67,800	313,400	16,800	670,400	256,800	307,300
Eastern Africa and Horn	555,200	4,900	245,900	260,200	73,300	83,700	20,900	100,300
Southeastern Africa	34,800	391,000	137,500	170,900	373,900	8,600	72,900	25,700
Central Southern Africa	125,600	60,700	34,200	212,300	93,400	406,800	759,800	19,500

Results and Discussion

During the 1982 to 1990 time period the eastern equatorial Pacific experienced two warm and two cold sea surface temperature episodes (Figure 1). Of these, the 1982-1983 ENSO cycle SST warming and the 1988-1989 ENSO cycle SST cooling were more pronounced. Our analysis identified sizeable areas of Africa, Australia, and South America where precipitation and hence our NDVI anomalies were associated with tropical Pacific SST anomalies (Table 1). South America and Australia were more directly associated with linked tropical Pacific SST and NDVI anomalies than was Africa (Figure 2).

We confirm previous analyses for Northeastern Brazil which have associated drought conditions with tropical Pacific SST warmings and excessive rainfall with tropical Pacific SST coolings [*Chu, 1991*]. We found areas ranging from 360,700 km^2 to 1,001,700 km^2 where NDVI/precipitation and SST anomalies were linked in northeastern Brazil. Furthermore, we found an inverse linear relationship between the NINO3 index and Northeastern Brazil NDVI anomalies (Figure 3). By contrast, southeastern South America experienced greater than average rainfall with tropical Pacific SST warmings; tropical Pacific SST coolings were associated with both excessive rainfall in March 1985 to February 1986 and severe drought in May 1988 to April 1989 (Table 1).

Eastern Australia was found to experience negative NDVI anomalies from both tropical Pacific SST warmings and coolings; the largest magnitude NDVI anomaly was indicative of a severe drought in 1982-1983 associated with the 1982-1983 tropical Pacific SST warming. We estimate an area of 1,743,500 km^2 was strongly associated with the 1982-1983 ENSO cycle SST warming event; by comparison, the ENSO cycle SST cooling in 1985-1986 and 1988-89 affected 744,400 km^2 and 549,900 km^2, respectively. The situation for central Australia is less clear; a major negative NDVI and precipitation shortfall anomaly occurred with the minor ENSO cycle SST cooling in 1985-1986, while other ENSO cycle SST anomaly events had positive and negative NDVI and hence rainfall anomalies [*Allan, 1991*]. In addition, Australian workers [*Foran and Pearce, 1989*] have reported a highly anomalous greening of central Australia associated with the 1988-1989 ENSO cycle SST cooling (Figure 4).

Africa, situated furthest from the tropical Pacific of the areas studied, was the least affected in terms of area of linked tropical Pacific SST and NDVI anomalies (Table 1). Our analysis identified three areas of Africa which were most strongly associated with linked tropical Pacific SST and co-

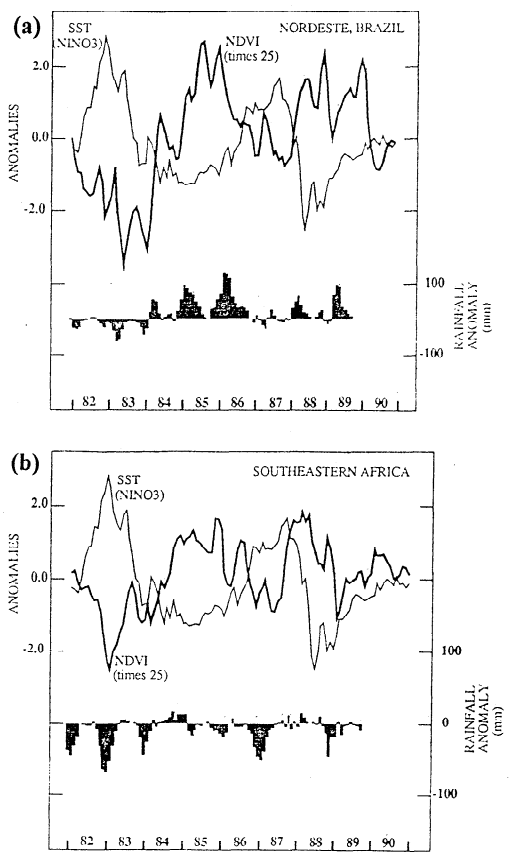

Figure 5. Time series plots for tropical Pacific SST and NDVI anomalies from 1982-1990. Also plotted at the bottom of each figure is the rainfall anomaly [*Dai and Fung, 1993*]. The NDVI time series is the average from pixels with two or more occurrences of significant association between SST and NDVI anomalies (cross correlation coefficients > |0.5|). The pixels are from an area within the regions shown in Figure 2: (a) Northeastern Brazil (2.6°S - 12°S × 36.4° W - 42.6°W) and (b) Southeastern Africa (Zimbabwe and Mozambique: 20.0°S - 25.0°N × 29.2°E - 33.8° E). The rainfall anomaly value is the average for the box.

incident NDVI anomalies: parts of Eastern Africa extending toward the Horn of Africa; Southeastern Africa; and Central Southern Africa.

Eastern Africa and the Horn of Africa showed a tendency toward wetter conditions with tropical Pacific SST warmings, which was more pronounced with the strong ENSO cycle SST warming of 1982-1983. Southeastern Africa experienced drought conditions in 1982-1983 associated with the ENSO cycle SST warming of that time and precipitation excess associated with the minor ENSO cycle SST cooling of 1985-1986; in both cases ≈400,000 km^2 of area was identified in our analysis for Southeastern Africa (Figure 5). The influence of eastern equatorial Pacific SST on vegetation in this region is so strong that Cane et al. have recently proposed forecasting Zimbabwean maize yields using NINO3 SST anomaly [*Cane et al., 1994*]. Central Southern Africa was most strongly associated with tropical Pacific SST coolings, but in an unpredictable fashion. ENSO cycle SST coolings in the 1980's were found to be associated with a positive NDVI or precipitation anomaly of 759,800 km^2, while the ENSO cycle SST cooling of 1985-1986 was associated with a negative NDVI or precipitation anomalies covering 406,800 km^2 (Table 1).

Our analysis confirms the disruptive effects of large-scale SST anomalies on regional-scale precipitation patterns and therefore vegetation in arid and semi-arid Africa, Australia, and South America for the time period of 1982-1990. While some areas such as Northeastern Brazil were consistently dryer during tropical Pacific SST warmings and consistently wetter during SST coolings, no comparable pattern was evident from the other areas identified by our analysis in Africa, Australia, and South America (Table 1). This must not be construed as true of all warm or cold events — 9 years is obviously too short a time period to estabish a pattern with statistical certainity. However, it is clear that tropical Pacific SST anomalies perturb continental precipitation patterns and therefore vegetation growth over large spatial scales.

Acknowledgements. The authors thank A. Dai and I. Fung for the rainfall anomaly data set and P. Schopf for the sea surface temperature data. The comments of two anonymous reviewers are greatly appreciated. This work has been supported by NASA's Mission to Planet Earth research program.

References

Allan, R. J., Australasia, in *Teleconnections Linking Worldwide Climate Anomalies*, edited by M. H. Glantz, R. W. Katz, and N. Nicholls, pp. 73-120, Cambridge Univ. Press, New York, 1991.

Asrar, G., M. Fuchs, E. T. Kanemasu, and J. L. Hatfield, Estimating absorbed photosynthetic radiation and leaf area index from spectral reflectance in wheat, *Agron. J.*, *76*, 300-306, 1984.

Cane, M. A., G. Eshel, and R. W. Bushland, Forecasting Zimbabwean maize yield using eastern equatorial Pacific sea surface temperature, *Nature*, *370*, 204-205, 1994.

Chu, P., Brazil's climate anomalies and ENSO, in *Teleconnections Linking Worldwide Climate Anomalies*, edited by M. H. Glantz, R. W. Katz, and N. Nicholls, pp. 43-72, Cambridge Univ. Press, New York, 1991.

Dai, A., and I. Y. Fung, Can climate variability contribute to the "missing" CO2 sink?, *Global Biogeochem. Cycles*, *7*, 599-606, 1993.

Foran, B., and G. Pearce, The Use of NOAA satellites and the green vegetation index to assess the 1988/89 summer growing season in central australia, *CSIRO Rangelands Research Report*, Alice Springs, Australia, 1989.

Fung, I. Y., C. J. Tucker, and K. C. Prentice, Application of advanced very high resolution radiometer vegetation index to study of atmosphere-biosphere exchange of CO2, *J. Geophys. Res.*, *92*, 2999-3015, 1987.

Los, S. O., C. O. Justice, and C. J. Tucker, A global 1 X 1 NDVI data set for climate studies derived from the GIMMS continental NDVI data, *Int. J. Remote Sens.*, *15*, 3493-3518, 1994.

Malo, A. R., and S. E. Nicholson, A study of rainfall and vegetation dynamics in the African Sahel using Normalized Difference Vegetation Index, *J. Arid Environ.*, *19*, 1-24, 1990.

McBride, J. L., and N. Nicholls, Seasonal relationships between Australian rainfall and the Southern Oscillation, *Mon. Wea. Rev.*, *111*, 1998-2004, 1983.

Nicholson, S. E., M. L. Davenport, and A. R. Malo, A comparision of the vegetation response to rainfall in the Sahel and East Africa, using Normalized Difference Vegetation Index from NOAA AVHRR, *Clim. Change*, *17*, 209-241, 1990.

Philander, S. G. H., Unusual conditions in the tropical Atlantic ocean in 1984, *Nature*, *322*, 236-238, 1986.

Press, W. H., B. P. Flannery, S. A. Teukolsky, and W. T. Vetterling, *Numerical Recipes*, 818pp, Cambridge University Press, Cambridge, 1986.

Ropelewski, C. F., and M. S. Halpert, Global and regional scale precipitation patterns associated with the El Niño/Southern Oscillation, *Mon. Wea. Rev.*, *115*, 1606-1626, 1987.

Ropelewski, C. F., and M. S. Halpert, Precipitation patterns associated with the high index phase of the Southern Oscillation, *J. Climate*, *2*, 268-284, 1989.

Sellers, P. J., Canopy reflectance, photosynthesis and transpiration, *Int. J. Remote Sens.*, *6*, 1335-1372, 1985.

Tucker, C. J., H. E. Dregne, and W. W. Newcomb, Expansion and contraction of the Sahara desert from 1980 to 1990, *Science*, *253*, 299-301, 1991.

Woodruff, S. D. *et al.* Comprehensive Ocean-Atmosphere Data Set (COADS) Release 1a: 1980-1992, NOAA, Washington, D.C., 1993.

R. B. Myneni, S. O. Los, C. J. Tucker, Biospheric Sciences Branch, Mail Code 923, NASA Goddard Space Flight Center, Greenbelt, MD 20771.

(Received July 10, 1995; revised January 10, 1996; January 16, 1996.)